Journal of Structural Chemistry. Vol. 54, No. 5, pp. 952-959, 2013

TAUTOMERISM OF SUBSTITUTED SALICYLALDEHYDE AND 2-DIPHENYLPHOSPHINEBENZALDEHYDE 1′-PHTHALAZINYLHYDRAZONES: X-RAY CRYSTALLOGRAPHY AND QUANTUM CHEMICAL MODELING

© **S. I. Levchenkov,[1] L. D. Popov,[2] I. N. Shcherbakov,[2] G. G. Aleksandrov,[3] A. A. Zubenko,[4] and V. A. Kogan[2]**

UDC 539.27:544.18:547.556.93

1′-Phthalazinylhydrazones of salicylaldehyde, its substituted derivatives, and 2-diphenylphosphinebenzaldehyde are synthesized and studied. A description is given of the structures salicylaldehyde 1′-phthalazinylhydrazone (**1a**) and 2-diphenylphosphinebenzaldehyde 1′-phthalazinylhydrazone (**2**), which exist in the crystal in the hydrazonophthalazone tautomeric form. Molecules of hydrazone **1a** form in the crystal infinite stacks of hydrogen bonded dimers with intermolecular π-stacking interactions. A quantum chemical calculation is made of the geometry and total energy of the possible tautomers in vacuum and in aqueous and chloroform solutions. The hydrazonophthalazone tautomers are shown to be the most stable in all cases. The X-ray crystallography results are compared with the calculated data.

DOI: 10.1134/S0022476613050168

Keywords: hydrazones, tautomerism, X-ray crystallography, hydrogen bond, density functional theory.

The reason for the interest in 1-hydrazinophthalazine (hydralazine) and its derivatives and their complexes with transition metals is the inherent biological activity of these compounds, especially their hypotensive, antiinflammatory, and anticancer activity [1-5]. An additional incentive is the fact that hydralazine metabolism involves the interaction with the carbonyl compounds formed in the Krebs cycle [6-8]. The literature describes several hydralazine hydrazones with a number of mono- and dicarbonyl compounds [9-16]. However, until recently there have been only two papers on salicylaldehyde 1′-phthalazinylhydrazones [17, 18] although hydrazones of salicylaldehyde and its substituted derivatives are “classical” ligand systems for modern coordination chemistry. It should be noted that these, as well as other studies, proceed from the assumption that 1′-phthalazinylhydrazones exist in the hydrazone tautomeric form. However, a number of studies using X-ray crystallography and quantum mechanical calculations have shown that the hydrazonophthalazone (diazine) tautomer is the main tautomeric form of this type of compounds [11, 14-16, 19, 20].

This paper presents the results of physicochemical studies and quantum chemical modeling of 1′-phthalazinyl-hydrazones of substituted salicylaldehydes (**1**) and 2-diphenylphosphinebenzaldehyde (**2**). The aldehyde component of the

[1]Southern Scientific Center, Russian Academy of Sciences, Rostov-on-Don, Russia; s.levchenkov@gmail.com. [2]Chemistry Department, Southern Federal University, Rostov-on-Don, Russia. [3]N. S. Kurnakov Institute of General and Inorganic Chemistry, Russian Academy of Sciences, Moscow, Russia. [4]North-Caucasian Zonal Research Veterinary Institute, Novocherkassk, Russia. Translated from *Zhurnal Strukturnoi Khimii*, Vol. 54, No. 5, pp. 914-922, September-October, 2013. Original article submitted February 2, 2013.

hydrazones were salicylaldehyde itself and its most synthetically accessible derivatives: 5-methoxy-, 5-bromo-, 5-nitro-, and 3,5-di-*tert*-butylsalicylic aldehydes.

EXPERIMENTAL

1′-Phthalazinylhydrazones of salicylaldehyde and its substituted derivatives of type **1** were synthesized according to the following procedure. An equivalent amount of sodium acetate was added to a hot suspension of 0.002 mol 1-hydrazinophthalazine hydrochloride in 40 ml ethanol, and then a hot solution of 0.002 mol of a given aldehyde in 10 ml ethanol was poured into the suspension. The reaction mixture was boiled for 1-3 h, after which 50 ml distilled water were added. The resulting precipitate was filtered and washed with water. Recrystallization from the ethanol–DMF mixture.

1a, R=H; m.p. 217°C. Elemental analysis: found, %: C 60.02, H 4.42, and N 20.94; for $C_{15}H_{12}N_4O$ calculated, %: C 68.17, H 4.58, and N 21.20. IR spectrum (ν, cm^{-1}): 3316 ν(OH), 3250 ν(NH), 1613, 1600 ν(C=N), 1270 ν(C–O). PMR spectrum (δ, ppm): 11.973 s (1H, NH), 10.355 s (1H, OH), 8.571 s (1H, CH_{arom}), 8.34 dd (1H, J_1 = 6.3 Hz, J_2 = 2.1 Hz, CH_{arom}), 7.965 s (1H, $CH_{azometh}$), 7.66 m (3H, CH_{arom}), 7.50 dd (1H, J_1 = 7.5 Hz, J_2 = 1.5 Hz, CH_{arom}), 7.21 td (1H, J_1 = 7.3 Hz, J_2 = 1.7 Hz, CH_{arom}), 6.87 m (2H, CH_{arom}).

1b, R=5-OCH_3; m.p. 194°C. Elemental analysis: found, %: C 65.18, H 4.82, and N 18.90; for $C_{16}H_{14}N_4O_2$ calculated, %: C 65.30, H 4.79, and N 19.04. IR spectrum (ν, cm^{-1}): 3308 ν(OH), 3280 ν(NH), 1609, 1590 ν(C=N), 1266 ν(C–O). PMR spectrum (δ, ppm): 12.178 s (1H, NH), 9.968 s (1H, OH), 8.655 s (1H, CH_{arom}), 8.30 dd (1H, J_1 = 7.2 Hz, J_2 = 1.5 Hz, CH_{arom}), 8.104 s (1H, $CH_{azometh}$), 7.75 m (3H, CH_{arom}), 7.57 d (1H, J = 2.4 Hz, CH_{arom}), 6.83 m (2H, CH_{arom}), 3.758 s (3H, CH_3).

1c, R=3,5-(*t*-Bu)$_2$; m.p. 221°C. Elemental analysis: found, %: C 73.57, H 7.60, and N 15.05; for $C_{23}H_{28}N_4O$ calculated, %: C 73.37, H 7.50, and N 14.88. IR spectrum (ν, cm^{-1}): 3300 ν(OH), 3255 ν(NH), 1611, 1598 ν(C=N), 1267 ν(C–O). PMR spectrum (δ, ppm): 12.193 s (1H, NH), 11.041 s (1H, OH), 8.660 s (1H, CH_{arom}), 8.30 d (1H, J = 7.5 Hz, CH_{arom}), 8.140 s (1H, $CH_{azometh}$), 7.75 м (3H, CH_{arom}), 7.33 d (1H, J = 2.1 Hz, CH_{arom}), 7.28 d (1H, J = 2.4 Hz, CH_{arom}), 1.438 s (9H, *t*-Bu), 1.278 s (9H, *t*-Bu).

1d, R=5-Br; m.p. > 250°C. Elemental analysis, found, %: C 62.75, H 3.53, and N 16.70; for $C_{15}H_{11}BrN_4O$ calculated, %: C 52.50, H 3.23, and N 16.33. IR spectrum (ν, cm^{-1}): 3272 ν(OH), 3190 ν(NH), 1619, 1601 ν(C=N), 1268 ν(C–O). PMR spectrum (δ, ppm): 12.308 s (1H, NH), 10.347 s (1H, OH), 8.613 s (1H, CH_{arom}), 8.34 d (1H, J = 2.9 Hz, CH_{arom}), 8.29 d (1H, J = 7.8 Hz, CH_{arom}), 8.125 s (1H, $CH_{azometh}$), 7.75 m (3H, CH_{arom}), 7.35 dd (1H, J_1 = 8.7 Hz, J_2 = 2.7 Hz, CH_{arom}), 6.85 d (1H, J = 8.7 Hz, CH_{arom}).

1e, R=5-NO_2; m.p. > 250°C. Elemental analysis, found, %: C 58.16, H 3.52, and N 22.81; for $C_{15}H_{11}N_5O_3$ calculated, %: C 58.25, H 3.58, and N 22.64. IR spectrum (ν, cm^{-1}): 3336 ν(OH), 3272 ν(NH), 1614, 1604 ν(C=N), 1286 ν(C–O). PMR spectrum (δ, ppm): 12.468 s (1H, NH), 11.65 s (1H, OH), 9.05 d (1H, J = 3.0 Hz, CH_{arom}), 8.705 s (1H, $CH_{azometh}$), 8.32 d (1H, J = 8.1 Hz, CH_{arom}), 8.172 s (1H, CH_{arom}), 8.12 dd (1H, J_1 = 9.0 Hz, J_2 = 2.7 Гц, CH_{arom}), 7.77 m (3H, CH_{arom}), 7.07 d (1H, J = 9.0 Hz, CH_{arom}).

1′-Phthalazinylhydrazone of 2-diphenylphosphinebenzaldehyde (2) was synthesized as follows. An equivalent amount of sodium acetate was added to a hot suspension of 0.03 mol 1-hydrazinophthalazine hydrochloride in 30 ml ethanol; the mixture was boiled for 10 min; and 0.3 mol 2-diphenylphosphinebenzaldehyde was added. The reaction mixture was refluxed for 4 h, after which 80 ml distilled water were added; the resulting mixture was left for a day. The yellow precipitate was filtered and washed with water and ethanol. Recrystallization from ethanol.

M.p. 190°C. Elemental analysis: found, %: C 75.13, H 5.01, and N 12.75; for $C_{27}H_{21}N_4P$ calculated, %: C 74.99, H 4.89, and N 12.96. IR spectrum (ν, cm^{-1}): 3250 ν(NH), 1621, 1600 ν(C=N). PMR spectrum (δ, ppm): 11.922 s (1H, NH), 8.95 d (1H, $J_{P–H}$ 4.5 Hz, CH=N), 8.5 m (1H, CH_{arom}), 8.23 d (1H, J 7.8 Hz, CH_{arom}), 8.121 s (1H, CH_{arom}), 7.7 m (3H, CH_{arom}), 7.4 m (8H, CH_{arom}), 7.2 m (4H, CH_{arom}), 6.7 m (1H, CH_{arom}).

TABLE 1. Crystallographic Data and Experiment and Refinement Details for Compounds **1a** and **2**

Parameter	Value	
	1a	**2**
Gross formula	$C_{15}H_{12}N_4O$	$C_{27}H_{21}N_4P$
Molecular mass	264.29	432.45
Crystal size, mm	0.32×0.12×0.12	0.26×0.18×0.12
Temperature, K	200(2)	173(2)
λ, Å	0.71073	0.71073
Crystal system	Triclinic	Triclinic
Space group	*P*-1	*P*-1
a, *b*, *c*, Å	6.7859(16), 8.3854(18), 11.777(3)	8.6512(7), 10.7550(8), 11.6520(9)
α, β, γ, deg	89.136(4), 82.840(4), 70.487(4)	84.6000(10), 87.6740(10), 89.2160(10)
V, Å^3	626.5(2)	1078.39(14)
Z	2	2
ρ(x), g/cm^3	1.401	1.332
μ, mm^{-1}	0.093	0.151
F(000)	276	452
θ data collection domain, deg	2.58-30.32	2.36-29.65
Reflection index ranges	$-9 \le h \le 9, -11 \le k \le 11, -16 \le l \le 16$	$-12 \le h \le 12, -15 \le k \le 14, -16 \le l \le 16$
Measured/independent reflections	7299/3682	11938/5998
Reflections with $I > 2\sigma(I)$	2638	4547
Number of refined parameters	181	289
R_1 ($I > 2\sigma(I)$)	0.0492	0.0378
wR_2 (all reflections)	0.1430	0.1095
GOOF	1.000	1.000
$\Delta\rho_{max}/\Delta\rho_{min}$, e/Å^{-3}	0.400/–0.326	0.376/–0.416
CSDB No.	904891	853334

The elemental analysis was conducted using a Perkin-Elmer 240C instrument. The PMR spectra were recorded in DMSO-d_6 using a Varian Unity 300 spectrometer (300 MHz) in the pulse Fourier mode, with HMDS used as an internal standard. The IR spectra were recorded using a Varian Scimitar 1000 FT-IR instrument in the domain 400-4000 cm^{-1}; the samples were prepared in the form of a suspension in paraffin oil.

X-Ray crystallographic study. Single crystals of compounds **1a** and **2** for XRD were obtained by slow cooling of the solutions in DMSO. The unit cell parameters and reflection intensities were measured with a Bruker Apex II diffractometer [21] with a CCD detector (MoK_α radiation, graphite monochromator, and ω scanning). The absorption of X-ray radiation was estimated semiempirically (T_{min}/T_{max} = 0.9489/0.9730) in the SADABS program [22]. The structures were solved by the direct method and refined by the full-matrix LSM in an anisotropic approximation for nonhydrogen atoms against F_{hkl}^2. Hydrogen atoms were put into geometrically calculated positions and refined in the rider model (U_{iso}(H) = 1.2U_{eq}(C) for all groups). All the calculations were made in the SHELX-97 programs [23]. The experiment details and crystallographic data are given in Table 1; selected interatomic distances and valence angles are given in Table 2; and the hydrogen bond characteristics are given in Table 3.

The quantum chemical calculations of the electronic and spatial structure of compound **1** were conducted in the GAUSSIAN′03 program [24] within the density functional theory (DFT) in vacuum and in aqueous and chloroform solutions. The solvent effect was considered within the polarizable continuum model (PCM) [25]. The calculations used the B3LYP hybrid exchange–correlation functional [26] with the exchange part in the form proposed by Becke [27] and the Lee–Yang–Parr

TABLE 2. Selected Interatomic Distances (Å) and Valence Angles (deg) in the Structure of **1a** and **2**

Bond	*d*	Bond	*d*	Bond	*d*
O(1)–C(1)	1.358(2)	P(1)–C(13)	1.8453(15)	N(4)–C(8)	1.370(2)
N(1)–C(7)	1.293(2)	C(13)–C(18)	1.418(2)	N(1)–C(19)	1.274(2)
N(1)–N(2)	1.3934(19)	C(18)–C(19)	1.459(2)	N(1)–N(2)	1.3981(17)
N(2)–C(8)	1.307(2)	C(6)–C(7)	1.447(2)	N(2)–C(20)	1.303(2)
P(1)–C(1)	1.8358(15)	N(3)–C(15)	1.287(2)	N(3)–C(20)	1.369(2)
P(1)–C(7)	1.8421(14)	N(3)–N(4)	1.3711(19)	N(3)–N(4)	1.361(2)
Angle	ω	Angle	ω	Angle	ω
C(7)–N(1)–N(2)	113.08(14)	C(7)–P(1)–C(13)	101.42(6)	N(2)–C(8)–C(9)	118.99(14)
C(8)–N(2)–N(1)	113.73(13)	C(1)–P(1)–C(7)	100.92(6)	N(4)–C(8)–C(9)	115.71(14)
C(15)–N(3)–N(4)	117.13(15)	C(18)–C(13)–P(1)	121.79(11)	N(2)–N(1)–C(19)	113.90(13)
C(8)–N(4)–N(3)	126.29(14)	N(1)–C(19)–C(18)	122.94(14)	N(1)–N(2)–C(20)	111.08(12)
O(1)–C(1)–C(2)	118.55(17)	O(1)–C(1)–C(6)	121.19(16)	N(2)–C(20)–N(3)	123.25(14)
C(1)–P(1)–C(13)	101.86(6)	N(2)–C(8)–N(4)	125.30(15)	N(4)–N(3)–C(20)	127.12(14)

TABLE 3. Characteristics of Hydrogen Bonds in Crystals of Compounds **1a** and **2**

D–H…A	D–H, Å	H…A, Å	D…A, Å	∠DHA, deg
		Compound **1a**		
O(1)–H(1)…N(1)	0.84	1.89	2.636(2)	147
N(4)–H(4A)…N(1)	0.88	2.34	2.666(2)	102
N(4)–H(4A)…N(3)^{i}	0.88	2.32	3.006(2)	134
		Compound **2**		
N(3)–H(3B)…P(1)	0.88	2.80	3.663(2)	169
N(3)–H(3B)…N(1)	0.88	2.20	2.563(2)	104

*Crystallographic positions: ^{i} $-x, -y+1, -z$.

correlation part [28]. The split-valence basis 6-311+G(*d*,*p*) was used as a basis set. The geometrical structure of the studied molecules was optimized for all the natural variables without any symmetry restrictions. Potential energy surface minima were identified for each structure by calculating the matrix of force constants and normal vibration frequencies. The ChemCraft program [29] was used to prepare the data and presentation images and visualize the calculated results.

RESULTS AND DISCUSSION

The mobility of NH protons in type **1** and **2** hydrazones explains the possibility of existence of the two main tautomeric forms: phthalazone (**A**) and hydrazone (**B**).

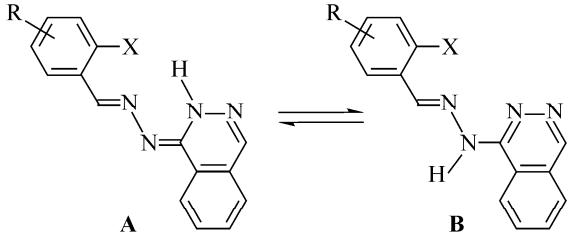

1, X = OH, R = H (**1a**), 5-OCH_3 (**1b**), 3,5-(t-Bu)$_2$ (**1c**), 5-Br (**1d**), 5-NO_2 (**1e**)
2, X = PPh_2, R = H

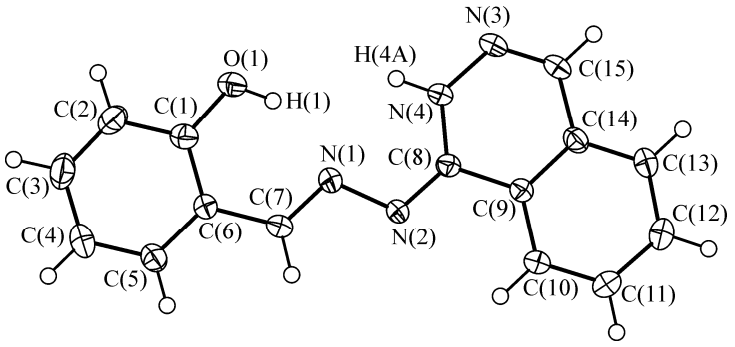

Fig. 1. Structure of hydrazone **1a** (50% probability thermal vibration ellipsoids).

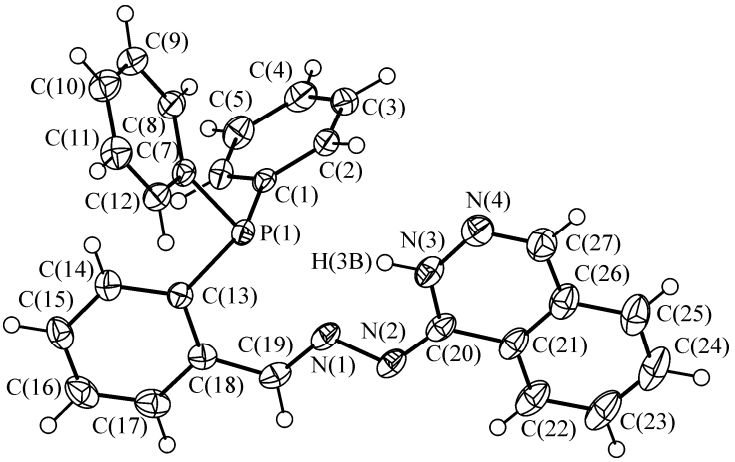

Fig. 2. Structure of hydrazone **2** (50% probability thermal vibration ellipsoids).

The fact that the NH proton signal in the PMR spectrum of hydrazones **1** and **2** is in a very weak field suggests that the compounds exist in the phthalazone tautomeric form (**A**), which is also typical of other hydrazinophthalazine hydrazones [11, 14-16, 19, 20]. This is also evidenced by the single crystal XRD data for salicylaldehyde 1′-phthalazinylhydrazone **1a** (Fig. 1) and 2-diphenylphosphinebenzaldehyde 1′-phthalazinylhydrazone **2** (Fig. 2).

Compound **1** crystallizes from DMSO in the hydrazone tautomeric form, which is evidenced by the lengths of the C–C and C–N bonds in the hydrazone and heterocyclic fragments [30]. In the crystal this form is stabilized by two intramolecular hydrogen bonds: the fairly strong O(1)–H(1)…N(1) bond, which closes the six-membered cycles, and the less strong N(4)–H(4A)…N(1) bond (Table 4). The molecule as a whole is not planar; the mean square planes of the phthalazine fragment (defined by the atoms N(3), N(4), and C(8)–C(15)) and benzene ring (the atoms C(1)–C(6)) form an angle of 15.27(8)° mostly due to the rotation around the =N–N= bond of the diazine chain (the dihedral angle C(7)=N(1)–N(2)=C(8) is 172.43(15)°) and, to a less extent, around the C(8)=N(2) bond (the dihedral angle N(1)–N(2)–C(8)–C(4) is 4.9(2)°). The mean square planes of the pyridazine and benzene cycles in the phthalazine fragment are slightly rotated relative to each other by an angle of 3.11(8)°.

The crystal packing of compound **1a** contains centrosymmetric hydrogen-bonded dimers, which are formed due to the formation of the bond pair H(4A)…N(3)^{i} and H(4A)^{i}…N(3) (symmetry code (i): (i: *–x*, *–y*+1, *–z*) between the phthalazine nitrogen atoms of neighboring hydrazone molecules (Table 4). These dimers are also observed to have one more pair of short contacts of the CH…O type formed by the atoms H(15A)…O(1)^{i} and H(15)^{i}…O(1) (d = 2.57 Å, which is less than the sum of the van der Waals radii by 0.15 Å). A number of π-stacking interactions are also observed between neighboring hydrazone

TABLE 4. Total Energy (au) and Relative Stability (ΔE, kcal/mol) of Tautomeric Forms of Substituted Salicylaldehyde and 2-Diphenylphosphinebenzaldehyde 1′-Phthalazinylhydrazones in Vacuum

Compound	R	Tautomeric form	
		Phthalazone (**A**)	Hydrazone (**B**)
1a	H	–873.2455254 (0.00)	–873.2278062 (11.12)
1b	5-OCH_3	–987.7988255 (0.00)	–987.7860817 (8.00)
1c	3,5-(*t*-Bu)$_2$	–1187.8332897 (0.00)	–1187.8152992 (11.29)
1d	5-Br	–3446.7869700 (0.00)	–3446.7705614 (10.30)
1e	5-NO_2	–1077.8113094 (0.00)	–1077.7910442 (12.72)
2	—	–1602.1716878 (0.00)	–1602.1591011 (7.90)

molecules. First, they are observed between the phthalazine fragments with the molecule in the crystallographic position 1–*x*, –*y*, –*z*, with the mutual orientation of the interacting molecules being such that the pyridazine cycle of one molecule is above the benzene cycle of the other molecule to complementarily compensate for distortions in the phthalazine fragment. The distance between the mean square planes of the cycles is 3.4766 Å for the benzene cycles and 3.4152(7) Å for the pyridazine cycles; the distance between the centroids of the benzene and pyridazine cycles is 3.5647(13) Å. Second, a π-stacking interaction is observed between the benzene rings of the salicyl aldiminate fragments with the molecule in the position 1–*x*, 1–*y*, 1–*z*. The distances between the mean square planes of the benzene rings are 3.4632(8) Å; the intercentroid distances are 3.7575(15) Å.

Hydrazone **2** also exists in the crystal in the phthalazone tautomeric form. The hydrogen atom H(3B) forms weak intramolecular hydrogen bonds with the atoms N(1) and P(1) (Table 4). In contrast to hydrazone **1a** and other phthalazinylhydrazones [5, 16, 19, 20], no intermolecular hydrogen bonds with the participation of the nitrogen atoms of the phthalazine fragment are formed in the case of compound **2**, which appears to be explained by steric hindrances created by the benzene rings of the diphenylphosphine substitute.

The benzene ring of the benzaldehyde fragment and the phthalazine cycle in the molecule of **2** are almost coplanar; the dihedral angle between their mean planes is 8.23(6)°. The mean planes of the carbon atoms C(1)–C(6) and C(7)–C(12) of the phenyl groups form angles of 88.61(8)° and 72.27(8)°, respectively, with the benzene ring plane of the benzaldehyde fragment; the dihedral angle between the mean planes of the phenyl groups is 87.96(8)°.

The intermolecular contacts established in the crystal lattice of hydrazone **2** include the fairly short hydrogen bonds of the type C–H…N that form the centrosymmetric dimers C(12)–H(12A)…N(2)^{ii} and C(12)^{ii}–H(12A)^{ii}…N(2) (symmetry code (ii): 1–*x*, 2–*y*, 1–*z*, $d_{H...N}$ = 2.52 Å, $d_{C...N}$ = 3.455(2) Å). The distance between the hydrogen and nitrogen atoms is less than the sum of the van der Waals radii by 0.23 Å.

To evaluate the relative stability of the tautomeric forms of hydrazones **1** and **2** in more detail, a quantum chemical calculation was made of the total energy and the electronic and spatial structure of the possible tautomers (the results are shown in Table 4).

The molecular structure of the most stable rotamers of hydrazone **1a** tautomeric forms is shown in Fig. 3.

According to the quantum chemical modeling results, the phthalazone tautomer **A** of hydrazone **1** is the most stable in vacuum for any substitutes R. The hydrazone tautomer **B** is destabilized with respect to the phthalazone one by approximately 8-13 kcal/mol. All the tautomers of type **1** compounds are observed to have a hydrogen bond between the phenol proton and the azomethine nitrogen atoms. It should be noted that the existence of a quinone tautomeric form [14] for salicylaldehyde hydrazones is virtually impossible; in the case of salicylaldehyde 1′-phthalazinylhydrazone, its energy in vacuum would be greater than that of the phthalazone tautomer by 26 kcal/mol. The energies of the most stable possible cyclic tautomers of compound **1** are greater by 13-14 kcal/mol than those of form **1a**. The relative stability of the tautomers of type **1** compounds is almost unchanged in aqueous and chloroform solutions: the phthalazone tautomers are the most stable, and the hydrazone ones are destabilized by 6-8 kcal/mol in water and by 7-11 kcal/mol in chloroform.

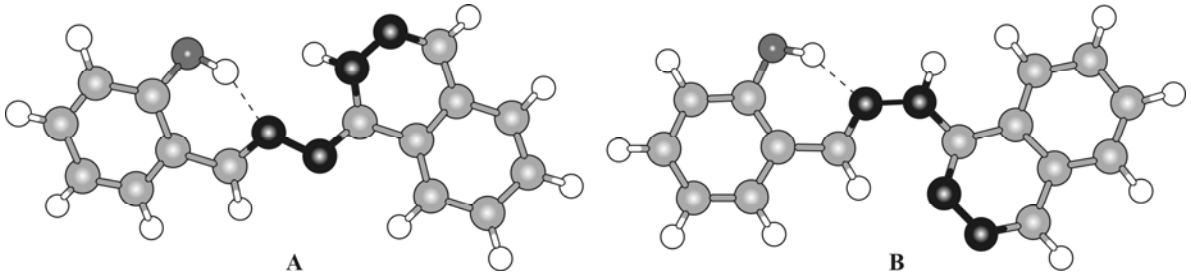

Fig. 3. Molecular structure of the tautomeric forms of hydrazone **1a** (R=H) in vacuum.

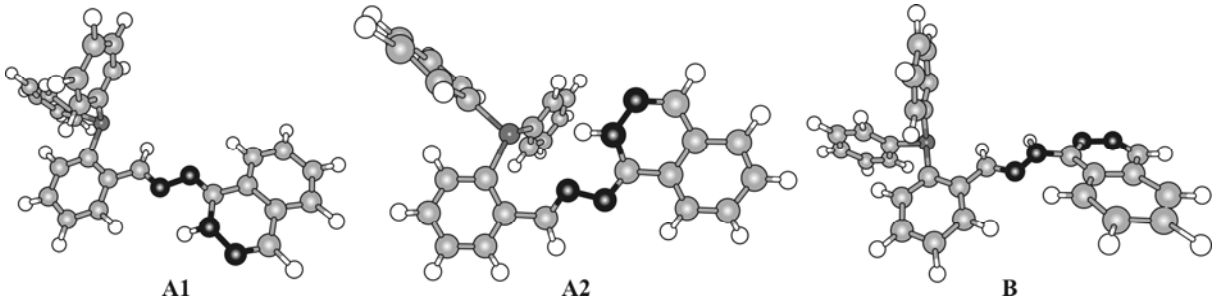

Fig. 4. Molecular structure of the tautomeric forms of hydrazone **2** in vacuum.

An almost similar pattern of relative tautomer stability is observed for hydrazone **2** (Table 4); the only difference is that other conformations of the tautomeric forms are the most stable (Fig. 4), which is explained by the repulsion of the undivided electron pairs of nitrogen and phosphorus atoms.

It should be noted that the total energy of conformer **A2** whose geometry is very similar to the structure of the molecule of **2** from the single-crystal XRD data, in vacuum is only 0.11 kcal/mol greater than that of the most stable form **A1**.

The relative stability of the studied forms of hydrazone **2** is the same in aqueous and chloroform solutions. The relative energies of conformer **A2** of the phthalazone form and the hydrazone tautomer are 1.84 kcal/mol and 5.98 kcal/mol in water and 0.51 kcal/mol and 6.60 kcal/mol in chloroform.

Thus, both for 1′-phthalazinylhydrazones of substituted salicylaldehydes and for 1′-phthalazinylhydrazone of 2-diphenylphosphinebenzaldehyde, the phthalazone tautomeric form is always more stable than the other tautomers.

It should be noted that the quantum chemical results for the spatial structure of the phthalazone tautomer of hydrazone **1a** are well consistent with those of the single-crystal XRD. The difference between the experimental and calculated lengths of the C–C and C–N bonds is always (for the molecule in vacuum, water, and chloroform) no greater than 0.01 Å. However, the best agreement is observed between the molecule geometry from the XRD data and the geometry calculated for the molecule in vacuum. The most substantial difference between the calculated geometry in vacuum and in solution is observed for the dihedral angle between the mean planes of the benzene ring and phthalazine cycle: 16.4° in vacuum, 26.9° in chloroform, and 33.4° in aqueous solution (15.3° from the XRD data).

In the case of hydrazone **2**, the calculated geometry of conformation **A2** of the phthalazone tautomer in vacuum is most close to the geometry from the XRD data (Fig. 4). There is a good agreement both between the bond lengths and valence angles and the dihedral angles between the cycles; in particular, the calculated dihedral angle between the mean planes of the benzene ring of the benzaldehyde fragment and the phthalazine cycle in vacuum is 12.2° (8.2° from the XRD data).

Thus, at quantum chemical modeling of the tautomeric forms of substituted salicylaldehyde and 2-diphenylphosphinebenzaldehyde 1′-phthalazinylhydrazones and the X-ray crystallographic study of salicylaldehyde and 2-diphenylphosphinebenzaldehyde 1′-phthalazinylhydrazone were accomplished; the results are compared with the calculated data. The hydrazonophthalazone tautomers are shown to be the most stable in all the cases.

REFERENCES

1. K. N. Zelenin, L. A. Khorseeva, and V. V. Alekseev, *Pharm. Chem. J*., **26**, No. 5, 395 (1992).
2. P. Vicini, M. Incerty, I. A. Doytchinova, et al., *Eur. J. Med. Chem*., **48**, No. 5, 624 (2006).
3. B. Segura-Pacheco, C. Trejo-Becerril, E. Perez-Cardenas, et al., *Clin. Cancer Res*., **9**, No. 5, 1596 (2003).
4. L. M. Kaminskas, S. M. Pyke, P. and C. Burcham, *J. Pharm. Exper. Therap*., **310**, No. 3, 1003 (2004).
5. V. A. Kogan, S. I. Levchenkov, L. D. Popov, and I. N. Shcherbakov, *Russ. J. Gen. Chem*., **79**, No. 1, 2767 (2009).
6. L. M. Kaminskas, S. M. Pyke, and P. C. Burcham, *Org. Biomol. Chem*., **18**, No. 2, 2578 (2004).
7. H. J. Knowles, Y. M. Tian, D. R. Mole, and A. L. Harris, *Circ. Res*., **95**, No. 2, 162 (2004).
8. P. A. Reece, *Med. Res. Rev*., **1**, No. 1, 73 (1981).
9. K. Nakashima, K. Shimada, and S. Akiyama*, Chem. Pharm. Bull*., **33**, No. 4, 1515 (1985).
10. T. Razvi, M. Ramalingam, and P. B. Sattur, *Ind. J. Chem. Sect. B*, **28**, No. 8, 987 (1989).
11. G. Giorgi, F. Ponticelli, L. Chiasserini, and C. Pellerano, *J. Chem. Soc., Perkin Trans. 2*, No. 11, 2259 (2000).
12. T. Odashima, M. Yamada, N. Yonemori, and H. Ishi, *Bull. Chem. Soc. Jpn*., **60**, No. 9, 3225 (1987).
13. L. D. Popov, I. N. Shcherbakov, S. I. Levchenkov, et al., *J. Coord. Chem*., **61**, No. 3, 392 (2008).
14. L. D. Popov, I. N. Shcherbakov, S. I. Levchenkov, et al., *Russ. J. Coord. Chem*., **37**, No. 7, 483 (2011).
15. L. D. Popov, S. I. Levchenkov, I. N. Shcherbakov, et al., *Russ. J. Gen. Chem*., **80**, No. 12, 2501 (2010).
16. L. D. Popov, S. I. Levchenkov, I. N. Shcherbakov, et al., *Russ. J. Gen. Chem*., **82**, No. 3, 465 (2012).
17. M. Callejon Mochon, M. Centero Gallego, and G. Perez, *Talanta*, **33**, No. 7, 627 (1986).
18. A. A. El-Sherif, M. M. Shoukry, and M. M. A. Abd-Elgawad, *Spectrochim. Acta A*, **98**, 307 (2012).
19. R. J. Butcher, J. P. Jasinski, H. S. Yathirajan, et al., *Acta Crystallogr*., **E63**, No. 9, o3674 (2007).
20. O. Büyükgüngör, M. Odabasoglu, A. M. Vijesh, and H. S. Yathirajan, *Acta Crystallogr*., **E63**, No. 10, o4084 (2007).
21. *Bruker APEX2 Software Package*, Bruker AXS, Madison (2005).
22. G. M. Sheldrik, *SADABS*, *Program for Scanning and Correction of Area Detector Data*, Univ. Göttingen, Germany (2004).
23. G. M. Sheldrick, *Acta Crystallogr. A*, **64**, No. 1, 112 (2008).
24. M. J. Frisch, G. W. Trucks, H. B. Schlegel, et al. *Gaussian 03*, *Revision D.01*, Gaussian, Inc., Wallingford CT (2004).
25. R. Cammi, B. Mennucci, and J. Tomasi, *J. Phys. Chem. A*, **104**, No. 23, 5631 (2000).
26. P. J. Stephens, F. J. Devlin, C. F. Chabalowski, and M. J. Frisch, *J. Phys. Chem*., **98**, No. 45, 11623 (1994).
27. A. D. Becke, *J. Chem. Phys*., **98**, No. 7, 5648 (1993).
28. C. Lee, W. Yang, and R. G. Parr, *Phys. Rev. B*, **37**, No. 2, 785 (1988).
29. G. A. Zhurko and D. A. Zhurko, *Chemcraft Version 1.6* (build 338): http://www.chemcraftprog.com.
30. F. H. Allen, O. Kennard, D. G. Watson, et al., *J. Chem Soc., Perkin Trans. 2*, No. 12, S1 (1987).